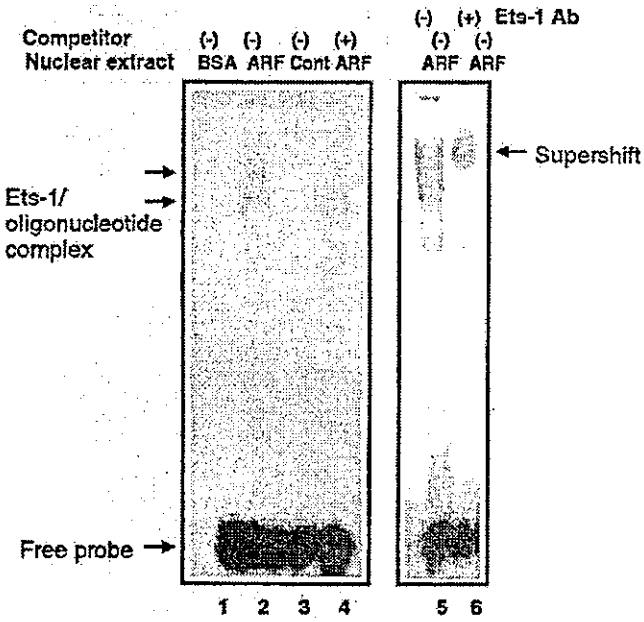


*Figure 7.* Electrophoretic mobility shift assay detected a protein binding to the promoter sequence of cyclin D1 in the nuclear extract of an ischemia-reperfusion rat kidney. A nuclear extract from renal cortex was prepared form the cortex of an ischemia-reperfusion rat kidney and a control rat kidney. The nuclear extract (10 $\mu$g) underwent a reaction in a premixed incubation buffer (gel shift assay kit) with a $\gamma$-$^{32}$P-end-labeled Ets-1 binding site of the cyclin D1 promoter lesion (5'-GATCTCGAGCAGGAAGTTCGA-3') for 30 min at 25°C. To establish the specificity of the reaction, we performed competition assays with 100-fold excess of unlabeled ets-1 biding oligonucleotides (heterologous competitor DNA). To perform supershift assay, we added 5 $\mu$g of anti–Ets-1 antibody (N-276, cs-111) to the nuclear extracts, incubated the extracts for 1 h at 4°C, and performed gel shift assay. Negative control without nuclear extract (lane 1), nuclear extract of ischemia-reperfusion kidney (lane 2), nuclear extract of control kidney (lane 3), and nuclear extract of ischemia-reperfusion kidney with 100-fold excess of unlabeled oligonucleotide (heterologous competitor DNA; lane 4) are shown. Nuclear extract of ischemia-reperfusion kidney incubated without anti–Ets-1 antibody (lane 5) and nuclear extract of ischemia-reperfusion kidney incubated with anti–Ets-1 (lane 6, supershift) are shown.

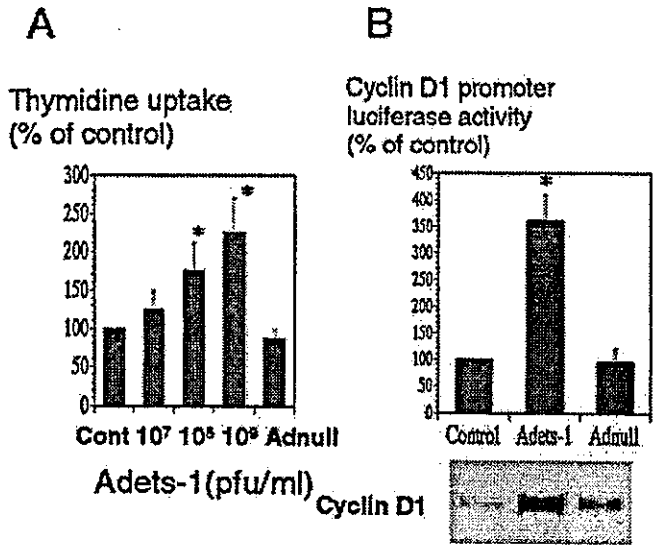


*Figure 8.* Cell proliferation and cyclin D1 expression by the overexpression of Ets-1 in LLC-PK1 cells. (A) We examined the effects of the overexpression of Ets-1 using an adenovirus on the cell proliferation of LLC-PK1 cells by [$^3$H]thymidine uptake. A shows the effects of Ets-1 on [$^3$H]thymidine uptake. (B) We next examined the role of Ets-1 in the regulation of cyclin D1 promoter activity and protein expression. We performed a transient transfection with the cyclin D1-luciferase reporter gene and the $\beta$-galactosidase expression vector and then infected it with either Adets-1 or Adnull ($10^9$ pfu/ml). When Ets-1 was overexpressed, cyclin D1 promoter activity increased significantly, by 3.6-fold, in LLC-PK1 cells; $n = 5$, mean ± SEM; $^*P <$ 0.05 *versus* control.

hypoxia causes the transcriptional stimulation of Ets-1 in LLC-PK1 cells *via* HIF-1$\alpha$, and that the overexpression of Ets-1 stimulates [$^3$H]thymidine uptake and cyclin D1 transcription in renal tubular cells.

Recovery from ARF requires the replacement of damaged cells with new cells that restore tubule epithelial integrity. Regeneration processes are characterized by the proliferation of dedifferentiated cells and subsequent redifferentiation of the daughter cells into the required cell phenotype. A similar phenomenon can also be observed during embryogenesis. Therefore, it was postulated that regeneration processes may repeat parts of the genetic program that serve during organogenesis to reestablish proper tissue function after damage (5,45). Recently, we reported that the developmental gene Wnt-4 is expressed in ischemic acute renal injuries and that Wnt-4 expression promotes the proliferation of renal tubular cells (26). This article suggested that some developmental genes are re-expressed during recovery of ARF. To confirm this hypothesis, we examined the expression patterns and function of Ets-1 in an ischemic acute renal model and in renal tubular cells.

In this study, we first demonstrated that Ets-1 expression is upregulated in the early phase of ischemic ARF. The Ets-1 expression was localized exclusively in the proximal tubule at the site of tubule regeneration where PCNA is expressed. These results suggest that Ets-1 protein may induce the transformation of regenerative renal tubular cells. During development, Ets-1 expression occurs in vascular structures and branching tissues, including the kidneys (18). In the adult kidney, the levels of Ets-1 expression are much lower than in the embryonic kidney (18,22). Thus, our data suggest that the cells that express Ets-1 after ischemic injury have characteristics of embryonic renal cells, such as in the mesenchymal-to-epithelial progression and proliferation.

Our data also indicate for the first time that Ets-1 signaling contributes to the activation of cyclin D1 promoter and protein expression. Sequences that resemble the core motif (GGA) required for Ets protein binding are located within the proximal cyclin D1 promoter (16). Overexpression of Ets-2 activates the

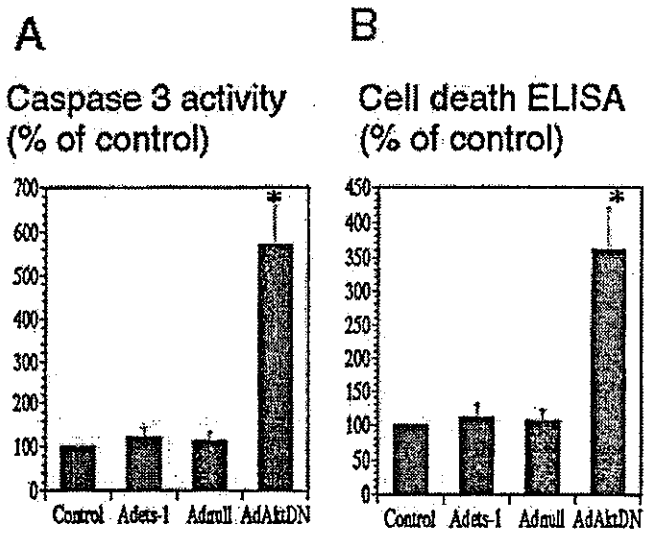


*Figure 9.* Apoptotic changes were not observed by the overexpression of Ets-1 in LLC-PK1 cells. We examined the effects of the overexpression of Ets-1 using an adenovirus on apoptotic changes of LLC-PK1 cells by caspase 3 activity and a cell death ELISA kit. AdAktDN was used as a positive control. Overexpression of AdAktDN stimulated caspase 3 activity (A) and the value of cell death ELISA (B). Overexpression of Adets-1 did not significantly change stimulated caspase 3 activity (A) or the value of cell death ELISA (B) in LLC-PK1 cells; $n = 5$, mean ± SEM; $^*P < 0.001$ *versus* control.

cyclin D1 promoter through the proximal 22 bp (46). The Ets-1 pathway plays a key role in normal embryonic development and in malignant vascular formation (17–20). However, the functional role of the Ets-1 signaling pathway in renal tubular cells is not well known. Our data demonstrate that overexpression of Ets-1 increases cyclin D1 promoter activity, protein expression, and cell-cycle progression in renal epithelial cells. If this is the case, then the expression of Ets-1 in the recovery phase of ARF could be expected to promote cell-cycle progression after tubular injury. Our data also demonstrated that the Ets-1 binding site of the cyclin D1 promoter binds to the nuclear extract of ischemic renal tissue. Our ischemia-reperfusion model also demonstrated that Ets-1 was co-localized with PCNA, suggesting that Ets-1 might be a proliferative signal in regenerating renal tubules.

In vascular endothelial cells, overexpression of Ets-1 caused apoptotic changes (32). Apoptosis of renal tubular cells is observed during ARF (47,48). Thus, we hypothesized that upregulated Ets-1 may cause apoptotic changes in renal tubular cells. To demonstrate this, we examined the effects of the overexpression of Ets-1 on apoptotic changes in LLC-PK1 cells. AdAktDN was used as a positive control, and overexpression of AdAktDN caused apoptotic changes in LLC-PK1 cells as shown in Figure 6. However, in our experimental conditions, the overexpression of Adets-1 did not significantly change caspase 3 activity or the value of cell death ELISA in LLC-PK1 cells. This result suggests that the apoptotic phenomenon caused by Ets-1 may be dependent on cell types or tissues. In the case of renal tubular cells, Ets-1 does not seem to play a role in apoptosis in ARF.

We have yet to see which kinds of mechanisms induce the transient upregulation of Ets-1 after ischemia-reperfusion acute renal injury. A recent paper by Oikawa *et al.* (27) reported that hypoxia induced Ets-1 *via* the activity of HIF-1α. In their study, the Ets-1 promoter contained a hypoxia-responsive element-like sequence, and HIF-1α bound to it under the hypoxic condition. The expression of HIF-1α was dramatically increased as early as 6 h after ischemia-reperfusion (Figure 1C). The upregulation of HIF-1α protein expression was temporary; the intensity of the Ets-1 band decreased at 48 and 72 h after ischemia-reperfusion. The time course of HIF-1α exceeded the time course of Ets-1. The hypoxic inducibility of the Ets-1 promoter assay is inhibited by the overexpression of dnHIF-1α in LLC-PK1 cells. The Western blot analysis also demonstrated that transfection of dnHIF-1α reduced the increase of Ets-1 protein by hypoxia (Figure 6C). These results indicated that the upregulation of Ets-1 by hypoxia is dependent on HIF-1α. This evidence led to the hypothesis that ischemia causes hypoxia in the renal tubule, and the hypoxic condition induces HIF-1α, then HIF-1α activates Ets-1 transcription in renal tubular cells. It will be of interest to examine which kinds of signal cascades exist between ischemia and Ets-1 induction. Further studies will be necessary to gain a more precise understanding of the molecular mechanisms of renal recovery after ischemia-reperfusion injury.

## Acknowledgments

An abstract of this work was presented at the 2003 Annual Meeting of the American Society of Nephrology, November 12–17, 2003, San Diego, CA.

We thank Dr. M. Eilers for providing the cyclin D1-promoter plasmid.

## References

1. Molitoris BA: Ischemic acute renal failure: Exciting times at our fingertips. *Curr Opin Nephrol Hypertens* 7: 405–406, 1998
2. Bonventre JV: Mechanisms of ischemic acute renal failure. *Kidney Int* 43: 1160–1178, 1993
3. Safirstein R, DiMari J, Megyesi J, Price P: Mechanisms of renal repair and survival following acute injury. *Semin Nephrol* 18: 519–522, 1998
4. Bacallao R, Fine LG: Molecular events in the organization of renal tubular epithelium: From nephrogenesis to regeneration. *Am J Physiol* 257: F919–F924, 1989
5. Wallin A, Zhang G, Jones TW, Jaken S, Stevens JL: Mechanism of the nephrogenic repair response. Studies on proliferation and vimentin expression after 35S-1,2-dichlorovinyl-L-cysteine nephrotoxicity in vivo and in cultured proximal tubule epithelial cells. *Lab Invest* 66: 474–484, 1992
6. Witzgall R, Brown D, Schwarz C, Bonventre JV: Localization of proliferating cell nuclear antigen, vimentin, c-fos, and clusterin in the postischemic kidney. *J Clin Invest* 93: 2175–2188, 1994
7. Safirstein R: Gene expression in nephrotoxic and ischemic acute renal failure. *J Am Soc Nephrol* 4: 1387–1395, 1994
8. Megyesi J, Udvarhelyi N, Safirstein RL, Price PM: The p53-independent activation of transcription of p21 WAF1/CIP1/SDI1 after acute renal failure. *Am J Physiol* 270: F1211–F1216, 1996

9. Megyesi J, Safirstein RL, Price PM: Induction of p21WAF1/CIP1/SDI1 in kidney tubule cells affects the course of cisplatin-induced acute renal failure. *J Clin Invest* 101: 777–782, 1998
10. Kato J, Matsushime H, Hiebert SW, Ewen ME, Sherr CJ: Direct binding of cyclin D to the retinoblastoma gene product (pRb) and pRb phosphorylation by the cyclin D-dependent kinase CDK4. *Genes Dev* 7: 331–342, 1993
11. Sherr CJ, Kato J, Quelle DE, Matsuoka M, Roussel MF: D-type cyclins and their cyclin-dependent kinases: G1 phase integrators of the mitogenic response. *Cold Spring Harb Symp Quant Biol* 59: 11–19, 1994
12. Terada Y, Nakashima O, Inoshita S, Kuwahara M, Sasaki S, Marumo F: TGF-beta-activating kinase-1 inhibits cell cycle and expression of cyclin D1 and A in LLC-PK1 cells. *Kidney Int* 56: 1378–1390, 1999
13. Laudet V, Hanni C, Stehelin D, Duterque CM: Molecular phylogeny of the ETS gene family. *Oncogene* 18: 1351–1359, 1999
14. Sharrocks AD: The ET: S-domain transcription factor family. *Nat Rev Mol Cell Biol* 2: 827–837, 2001
15. Sharrocks AD, Brown AL, Ling Y, Yates PR: The ETS-domain transcription factor family. *Int J Biochem Cell Biol* 29: 1371–1387, 1997
16. Wasylyk B, Hahn SL, Giovane A: The Ets family of transcription factors. *Eur J Biochem* 211: 7–18, 1993
17. Ito M, Nakayama T, Naito S, Matsuu M, Shichijo K, Sekine I: Expression of Ets-1 transcription factor in relation to angiogenesis in the healing process of gastric ulcer. *Biochem Biophys Res Commun* 246: 123–127, 1998
18. Kola I, Brookes S, Green AR, Garber R, Tymms M, Papas TS, Seth A: The Ets-1 transcription factor is widely expressed during murine embryo development and is associated with mesodermal cells involved in morphogenetic processes such as organ formation. *Proc Natl Acad Sci U S A* 90: 7588–7592, 1993
19. Hultgardh NA, Cercek B, Wang JW, Naito S, Lovdahl C, Sharifi B, Forrester JS, Fagin JA: Regulated expression of the ets-1 transcription factor in vascular smooth muscle cells in vivo and in vitro. *Circ Res* 78: 589–595, 1996
20. Naito S, Shimizu S, Maeda S, Wang J, Paul R, Fagin JA: Ets-1 is an early response gene activated by ET-1 and PDGF-BB in vascular smooth muscle cells. *Am J Physiol* 274: C472–C480, 1998
21. Maroulakou IG, Bowe DB: Expression and function of Ets transcription factors in mammalian development: A regulatory network. *Oncogene* 19: 6432–6442, 2000
22. Maroulakou IG, Papas TS, Green JE: Differential expression of ets-1 and ets-2 proto-oncogenes during murine embryogenesis. *Oncogene* 9: 1551–1565, 1994
23. Naito T, Razzaque MS, Nazneen A, Liu D, Nihei H, Koji T, Taguchi T: Renal expression of the Ets-1 proto-oncogene during progression of rat crescentic glomerulonephritis. *J Am Soc Nephrol* 11: 2243–2255, 2000
24. Reisdorff J, En-nia A, Stefanidis I, Floege J, Lovett DH, Mertens PR: Transcriptional factor Ets-1 regulates gelatinase A gene expression in mesangial cells. *J Am Soc Nephrol* 13: 1568–1578, 2002
25. Imgrund M, Grone E, Grone HJ, Kretzler M, Holzman L, Schlondorff D, Rothenpieler UW: Re-expression of the developmental gene Pax-2 during experimental acute tubular necrosis in mice. *Kidney Int* 56: 1423–1431, 1999
26. Terada Y, Tanaka H, Okado T, Shimamura H, Inoshita S, Kuwahara M, Sasaki S: Expression and function of the developmental gene Wnt-4 during experimental acute renal failure in rats. *J Am Soc Nephrol* 14: 1223–1233, 2003
27. Oikawa M, Abe M, Kurosawa H, Hida W, Shirato K, Sato Y: Hypoxia induces transcription factor ETS-1 via the activity of hypoxia-inducible factor-1. *Biochem Biophys Res Commun* 289: 39–43, 2001
28. Raouf A, Li V, Kola I, Watson DK, Seth A: The Ets1 proto-oncogene is upregulated by retinoic acid: Characterization of a functional retinoic acid response element in the Ets1 promoter. *Oncogene* 19: 1969–1974, 2000
29. Solomon DL, Philipp A, Land H, Eilers M: Expression of cyclin D1 mRNA is not upregulated by Myc in rat fibroblasts. *Oncogene* 11: 1893–1897, 1995
30. Tanaka T, Hanafusa N, Ingelfinger JR, Ohse T, Fujuta T, Nangaku M: Hypoxia induces apoptosis in SV40-immortalized rat proximal tubular cells through the mitochondrial pathways, devoid of HIF1-mediated upregulation of Bax. *Biochem Biophys Res Commun* 309: 222–231, 2003
31. Halterman MW, Miller CC, Federoff HJ: Hypoxia-inducible factor-1a mediates hypoxia-induced delayed neuronal death that involves p53. *J Neurosci* 19: 6818–6824, 1999
32. Teruyama K, Abe M, Nakano T, Iwasaka YC, Takahashi S, Yamada S, Sato Y: Role of transcription factor Ets-1 in the apoptosis of human vascular endothelial cells. *J Cell Physiol* 188: 243–252, 2001
33. Terada Y, Inoshita S, Hanada S, Shimamura H, Kuwahara M, Ogawa W, Kasuga M, Sasaki S, Marumo F: Hyperosmolality activates Akt and regulates apoptosis in renal tubular cells. *Kidney Int* 60: 553–567, 2001
34. Terada Y, Okado T, Inoshita S, Hanada S, Kuwahara M, Sasaki S, Yamamoto T, Marumo F: Glucocorticoids stimulate $p21^{CIP1}$ and arrest cell cycle in vitro and in anti-GBM glomerulonephritis. *Kidney Int* 59: 1706–1716, 2001
35. Denker BM, Smith BL, Kuhajda FP, Agre P: Identification, purification, and partial characterization of a novel Mr 28,000 integral membrane protein from erythrocytes and renal tubules. *J Biol Chem* 263: 15634–15642, 1988
36. Yamamoto T, Sasaki S: Aquaporins in the kidney: Emerging new aspects. *Kidney Int* 54: 1041–1051, 1998
37. Nielsen S, Agre P: The aquaporin family of water channels in kidney. *Kidney Int* 48: 1057–1068, 1995
38. Terada Y, Tomita K, Homma MK, Nonoguchi H, Yang T, Yamada T, Yuasa Y, Krebs EG, Sasaki S, Marumo F: Sequential activation of Raf-1 kinase, mitogen-activated protein (MAP) kinase kinase, MAP kinase, and S6 kinase by hyperosmolality in renal cells. *J Biol Chem* 269: 31296–31301, 1994
39. Okado T, Terada Y, Tanaka H, Inoshita S, Nakao A, Sasaki S: Smad7 mediates transforming growth factor-β-induced apoptosis in mesangial cells. *Kidney Int* 62: 1178–1186, 2002
40. Terada Y, Tomita K, Nonoguchi H, Yang T, Marumo F: Different localization and regulation of two types of vasopressin receptor messenger RNA in microdissected rat nephron segments using reverse transcription polymerase chain reaction. *J Clin Invest* 92: 2339–2345, 1993
41. Fort P, Marty L, Piechaczyk M, El SS, Dani C, Jeanteur P, Blanchard JM: Various rat adult tissues express only one major mRNA species from the glyceraldehyde-3-phosphate-dehydrogenase multigenic family. *Nucleic Acids Res* 13: 1431–1442, 1985
42. Gibson UE, Heid CA, Williams PM: A novel method for real time quantitative RT-PCR. *Genome Res* 6: 995–1001, 1996

43. Heid CA, Stevens J, Livak KJ, Williams PM: Real time quantitative PCR. *Genome Res* 6: 986–994, 1996
44. Terada Y, Yamada T, Nakashima O, Tamamori M, Ito H, Sasaki S, Marumo F: Overexpression of cell cycle inhibitors (p16INK4 and p21Cip1) and cyclin D1 using adenovirus vectors regulates proliferation of rat mesangial cells. *J Am Soc Nephrol* 8: 51–60, 1997
45. Bacallao R, Fine LG: Molecular events in the organization of renal tubular epithelium: From nephrogenesis to regeneration. *Am J Physiol* 257: F913–F924, 1989
46. Albanese C, Johnson J, Watanabe G, Eklund N, Vu D, Arnold A, Pestell RG: Transforming p21ras mutants and c-Ets-2 activate the cyclin D1 promoter through distinguishable regions. *J Biol Chem* 270: 23589–23597, 1995
47. Shimizu A, Yamanaka N: Apoptosis and cell desquamation in repair process of ischemic tubular necrosis. *Virchows Arch B Cell Pathol Incl Mol Pathol* 64: 171–180, 1993
48. Ueda N, Kaushal GP, Shah SV: Apoptotic mechanisms in acute renal failure. *Am J Med* 108: 403–415, 2000

Original Report: Laboratory Investigation

American Journal of Nephrology

Am J Nephrol 2004;24:188–197
DOI: 10.1159/000076758

Received: September 30, 2003
Accepted: January 4, 2004
Published online: February 12, 2004

# Different Type and Localization of CD44 on Surface Membrane of Regenerative Renal Tubular Epithelial Cells in vivo

Yuansheng Xie[a,c] Shinichi Nishi[a] Sachiko Fukase[a] Hiroaki Nakamura[b]
Xiangmei Chen[c] Naofumi Imai[a] Minoru Sakatsume[a] Akihiko Saito[a]
Mitsuhiro Ueno[a] Ichiei Narita[a] Toshio Yamamoto[b] Fumitake Gejyo[a]

[a]Division of Clinical Nephrology and Rheumatology, Niigata University Graduate School of Medical and Dental Sciences, Niigata, and [b]Department of Oral Morphology, Science of Functional Recovery and Reconstruction, Okayama University Graduate School of Medicine and Dentistry, Okayama, Japan; [c]Kidney Center of PLA, Department of Nephrology, Chinese General Hospital of PLA, Beijing, China

**Key Words**
Acute tubular necrosis · CD44 · Plasma membrane

**Abstract**
***Background:*** CD44 is a transmembrane glycoprotein comprising an extracellular domain, a transmembrane domain, and a cytoplasmic tail. Previous studies demonstrated that CD44 was generally restricted to lateral-basal plasma membrane (PM) of epithelial cells, whether it localized on apical PM in vivo has not been clarified. ***Methods:*** In this study, we used a gentamicin-induced acute tubular necrosis (ATN) and spontaneous recovery model in rats and two distinct antibodies, an anti-rat distal extracellular domain (OX49) of standard CD44 (CD44-OX49) and an anti-rat CD44 cytoplasmic tail (CD44CPT), to survey the localization of CD44-OX49 and CD44CPT on the PM in renal tubular epithelial cells in different recovery stages after ATN with immunohistochemistry and immunoelectron-microscopic examinations. ***Results:*** CD44-OX49 was localized not only on the lateral-basal PM in tubular epithelial cells, but also on the apical surface membrane in PCNA-positive newly regenerative tubular epithelial cells in early recovery stages after ATN. However, CD44CPT was only localized on the lateral-basal PM. The immunoelectron-microscopic results showed that CD44-OX49 localization was changed from the apical to lateral to basal surface membrane in renal tubular epithelial cells during the recovery process after ATN, finally disappearing from basal PM when normal polarized epithelial cells formed. ***Conclusions:*** These results suggest that there were two types of CD44 including CD44 without a cytoplasmic tail localizing on the apical surface membrane related to newly regenerative epithelial cells, and CD44 with a cytoplasmic tail localizing on the lateral-basal PM related to establishment of tubular epithelial cell polarity after ATN in vivo.



KARGER
Fax + 41 61 306 12 34
E-Mail karger@karger.ch
www.karger.com


0250–8095/04/0242–0188$21.00/0

Accessible online at:
www.karger.com/ajn

Prof. Fumitake Gejyo
Division of Clinical Nephrology and Rheumatology
Niigata University Graduate School of Medical and Dental Sciences
1-757 Asahimachi-dori, Niigata 951-8510 (Japan)
Tel. +81 25 227 2200, Fax +81 25 227 0775, E-Mail gejyo@med.niigata-u.ac.jp

## Introduction

The surface of polarized epithelial cells such as renal tubular epithelial cells is typically divided into two functionally and biochemically distinct, but physically continuous, domains separated by junctional complexes, termed apical and lateral-basal (also known as basolateral) plasma membrane (PM) domains [1]. The apical PM, facing the organ lumen, has a protective role by acting as a barrier between the external and internal environments and contains the necessary transporters for the uptake of small molecules. The lateral-basal PM is involved in cell-cell and cell-matrix adhesion, and also contains biological molecules involved in signal transduction and nutrient uptake [2].

CD44 is a broadly distributed multistructural and multifunctional transmembrane glycoprotein. It has at least 20 multiple isoforms of different molecular sizes (85–230 kD), such as standard CD44 or hemotopietic CD44, variant CD44 and epithelial CD44. The major physiological role of CD44 is to maintain organ and tissue structure via cell-cell and cell-matrix adhesion, while it is also involved in cell motility and migration, differentiation, cell signaling and gene transcription [3]. The CD44 protein is a single chain molecule comprising an N-terminal extracellular domain, a transmembrane domain, and a cytoplasmic tail [4]. The cytoplasmic tail of CD44 contributes to ligand and cytoskeletal associated protein binding, and determines membrane localization in polarized epithelial cells [5, 6]. In vitro studies have demonstrated that in polarized Madin-Darby canine kidney (MDCK) epithelial cell cultures, a tailless CD44 molecule is localized on the apical PM, whereas wild-type CD44 is restricted to the lateral-basal PM of epithelial cells, suggesting that the localization of CD44 may be regulated [7]. However, in vivo studies demonstrated that CD44 is generally localized on the lateral-basal PM of renal tubular polarized epithelial cells [8], and it remains unclear whether CD44 is also localized on the apical PM of tubular epithelial cells in any pathophysiological condition and the structure of CD44 located on distinct surface membrane of tubular epithelial cells in vivo.

Our previous study showed the up-regulated expression of CD44 in renal tubules during the recovery process after acute tubular necrosis (ATN) [9], but the exact localization and distribution of CD44 during the process of injury and repair of the kidneys remains poorly understood. In this study, we used a gentamicin-induced ATN and spontaneous recovery model in rats and two distinct antibodies, an anti-rat distal extracellular domain (OX49) of standard CD44 (CD44-OX49) and an anti-rat CD44 cytoplasmic tail (CD44CPT), surveyed the different localization of CD44-OX49 and CD44CPT in the surface membranes of renal tubular epithelial cells in different recovery stages after ATN and discussed the potential roles of CD44 localized on different surface membrane.

## Methods

*Animal Examination*

Experiments were performed on 32 male Wistar rats (Charles River Japan, Yokohama, Japan) weighing between 220 and 250 g that were divided into two groups: a gentamicin group including 20 rats and a control group including 12 rats. The rats in the gentamicin group were given 150 mg/kg/day of gentamicin sulphate solution (Sigma-Aldrich Co. St. Louis, Mo., USA) by subcutaneous injection in the neck for 5 days, and the rats in the control group were given an equal volume of normal saline instead. All animals were fed a diet of standard laboratory chow and allowed free access to water, but were deprived of water for 24 hours before the first gentamicin administration, and for 12 hours a day during gentamicin administration. Five rats in the gentamicin group and 3 rats in the control group were sacrificed under ether anesthesia on days 6, 10, 15, and 30 after the first gentamicin injection, respectively. The left kidney of each rat was removed and bisected for routine histological examination by general light microscopy and general electron microscopy. Then, each rat was infused with 4% paraformaldehyde from the abdominal aorta and the right kidney was removed and bisected for immunohistochemical and immunoelectron-microscopic examination.

*Primary Antibodies*

The following primary antibodies were used in this study: a purified mouse anti-rat CD44H (also known as CD44s; clone: OX-49, a distal extracellular domain of standard CD44, named as CD44-OX49 by the author) monoclonal antibody (PharMingen, San Diego, Calif., USA), a purified rabbit anti-rat CD44 cytoplasmic tail (CD44CPT) antibody (see below) and a mouse anti-proliferating cell nuclear antigen (PCNA) monoclonal antibody (Dako, Glostrup, Denmark).

According to a previous report, residues 423–503 of rat CD44 were located in the cytoplasmic region [10]. An antibody against rat CD44CPT was constructed using the following procedure. A cysteine-conjugated peptide corresponding to residues 483–503 (DQFMTADETRNLQSVDMKIGV) of rat CD44 was synthesized and coupled via a terminal cysteine residue to keyhole limpet hemocyanin. This antigen was subcutaneously injected into rabbits and antisera were collected. A specific antibody to CD44CPT was purified with Affi-Gel 10 (Bio-Rad, Hercules, Calif., USA) coupled with the peptide. The antibody test for CD44CPT showed that the antibody prepared against CD44CPT was stable and special in its activity to CD44CPT.

The antibodies against rat CD44-OX49 and CD44CPT needed not any special antigen retrieval techniques in their use.

*Immunohistochemistry*

Immunohistochemical staining was carried out on 3-μm wax sections. The sections were first dewaxed and dehydrated. Then, they

were incubated with 0.6% $H_2O_2$ in methanol for 30 min to eliminate endogenous peroxidase activity and incubated with normal goat serum (Chemicon, Temecula, Calif., USA) at room temperature for 30 min to block non-special reaction. Subsequently, they were incubated at 4°C for 24 h with primary antibodies, mouse anti-rat CD44-OX49 (2.5 μg/ml) or rabbit anti-CD44CPT (1.5 μg/ml) or mouse anti-PCNA (1:20). After washing in PBS for 3 × 5 min, the sections were incubated with a secondary antibody (Dako, EnVision+™, Carpinteria, Calif., USA), goat anti-mouse IgG (for CD44-OX49) or goat anti-rabbit IgG (for CD44CPT) conjugated with peroxidase, or goat anti-mouse IgG conjugated with alkaline phosphatase (for PCNA), at room temperature for 30 min. After washing with PBS, the sections were incubated with a DAB peroxidase substrate solution (Nichirei, Tokyo, Japan) or a Fuchsin alkaline phosphatase substrate solution (Dako, Carpinteria, Calif., USA) with an endogenous alkaline phosphatase inhibitor (Dako). The cellular nuclei of the sections were counterstained with hematoxylin. Normal mouse IgG and normal rabbit IgG were used as negative controls, respectively (Santa Cruz Biotechnology, Calif., USA).

*Double Staining*

Double staining was performed on the same tissue section, which included a combination of CD44-OX49 immunohistochemistry and PCNA immunohistochemistry (see above) as a marker of cell proliferation or regeneration. The first immunostaining for CD44-OX49 was performed with a DAB peroxidase substrate solution, which caused a brown color reaction, followed by washing in PBS for 3 × 5 min and treatment for 10 min in a microwave oven in a 0.01 *M* citrate buffer (pH 6.0). Then, the second immunostaining for PCNA was performed with a Fuchsin alkaline phosphatase substrate solution, which caused a red color reaction.

*Immunoelectron-Microscopic Examination*

After perfusion fixation with 4% paraformaldehyde, each rat kidney was removed, cut into some small blocks (2 × 2 × 2 mm) and taken into fusion fixated with 4% phosphate buffered paraformaldehyde and 0.01% glutaraldehyde for 2–4 h at 4°C. The tissue was then washed overnight in a 0.1 *M* phosphate buffer (PB), and washed further in graded 10, 15 and 20% sucrose PBS series for 24 h at 4°C, respectively. After rinsing in a mixed solution of 20% sucrose and 8% glycerin PBS for 2 h at 4°C, the tissue was embedded with optimal cutting temperature (OCT) compound in acetone and dry ice ethanol. Approximately 10–20 μm frozen sections were obtained with a frozen microslicer. Then, according to the above immunohistochemical staining procedure, the sections were preincubated with 0.6% $H_2O_2$ in methanol and normal goat serum for 30 min at room temperature, respectively, and incubated with a purified mouse anti-rat CD44-OX49 monoclonal antibody (2.5 μg/ml) for 24 h at 4°C, followed by a goat anti-mouse second antibody conjugated with peroxidase for 30 min. After washing with PBS, the sections were incubated with a DAB peroxidase substrate solution. After postfixation with 2% osmium tetroxide ($OsO_4$) in 0.1 *M* PB for 2 h, the specimens were dehydrated in a graded 50, 60, 70, 80, 90 and 100% (three times) ethanol series for 10 min, respectively, embedded in epoxy resin (Epok 812; Oken, Tokyo, Japan) and polymerized at 60°C for 5 days. Ultrathin sections with 90–100 nm were obtained and half of the sections were stained with lead citrate for 3 min and observed under a H-7100 transmission electron microscope (Hitachi, Tokyo, Japan) at an accelerating voltage of 75 kV.

*Quantitative Analysis*

Quantitative analysis was performed to investigate the distribution of CD44 on epithelial cell PM in distinct stages in gentamicin-induced ATN and its recovery process. Observations were performed on 100 non-overlapping random tubules 20 per rat kidney section from 5 rats at days 6, 10, 15 and 30 after the first gentamicin administration. Day 6, 100 totally necrotic tubules stained with CD44-OX49; day 10, 100 tubules with PCNA positive staining – these tubules were stained using the double staining technique PCNA and CD44-OX49; day 15 and day 30, 100 tubules with CD44-OX49 positive staining. The number of CD44-OX49-positive stained tubules with stained cells greater than 50% of PM was recorded. If both the basolateral PM and the apical PM were stained in greater than 50% cells these were recorded separately as basolateral PM positive and apical PM positive. If the tubules were not fully necrotic in tubules on day 6, tubules which were PCNA-negative on day 10 or tubules with less than 50% cells stained for CD44-OX49 were not recorded as positive tubules.

## Results

*Histopathological Findings*

As described previously [9], renal proximal tubular necrosis appeared to develop on day 6 (day 1–5 administration of gentamicin) in the gentamicin group. On day 10, there was a lot of desquamated epithelial cell debris in the dilated tubular lumens. Mononuclear cells infiltrated interstitial regions and tubular lumens from the superficial cortex to the corticomedullary zone. Newly regenerative tubular epithelial cell lines appeared along the tubular

**Fig. 1.** Localization of distal extracellular domain (OX49) of standard CD44 (CD44-OX49) and CD44 cytoplasmic tail (CD44CPT). Sections labelled **a**, **c**, **e**, and **g** show immunohistochemical staining of CD44-OX49 (brown) and cellular nuclear staining at days 6, 10, 15, and 30 after the first gentamicin administration (150 mg/kg/day × 5), respectively. Serial sections **b**, **d**, **f**, and **h** show immunohistochemical staining of CD44CPT (brown) and cellular nuclear staining at days 6, 10, 15 and 30 after the first gentamicin administration, respectively. On day 6, CD44-OX49 (arrow, **a**) and CD44CPT (arrow, **b**) are negative in the desquamated epithelia, denuded tubular basement membranes. CD44-OX49 and CD44CPT are positive in only non-necrotic tubules. On day 10, CD44-OX49 is markedly positive on the apical plasma membrane (PM) in newly regenerative epithelial cells (arrow, **c**), whereas CD44CPT is negative on the same apical PM (arrow, **d**). On day 15, CD44-OX49 (arrow, **e**) and CD44CPT (arrow, **f**) are almost identically located on the lateral PM. On day 30, CD44-OX49 (arrow, **g**) and CD44CPT (arrow, **h**) are almost identically expressed on the basal PM in non-full recovery tubular epithelial cells, but are negative in normal or full recovery tubular epithelial cells (triangle, **g** and **h**, respectively). Original magnification × 100.

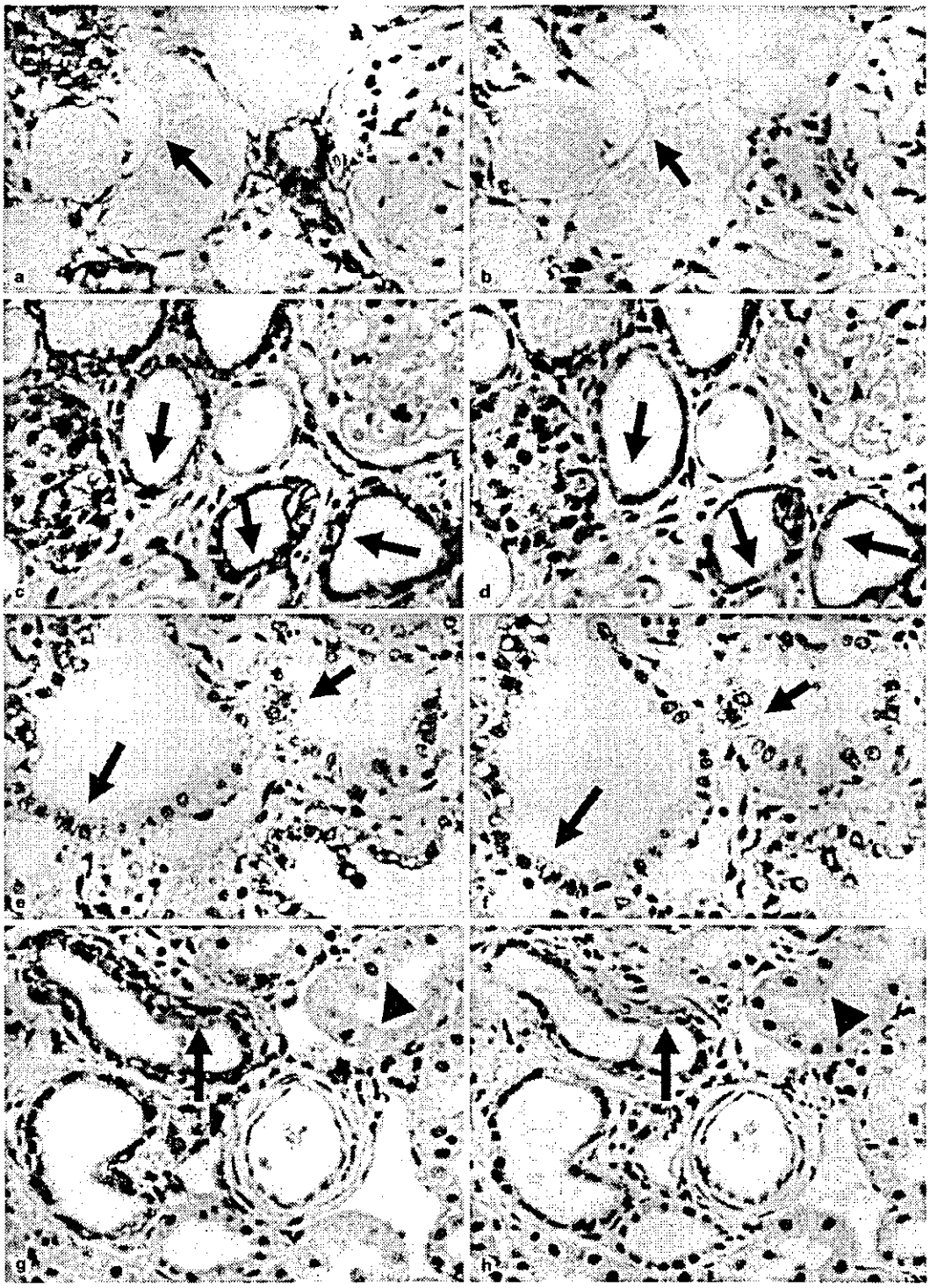
a
b
c
d
e
f
g
h

basement membranes. On day 15, the regenerative tubular epithelial cells became larger and the renal tubular epithelium became thicker. On day 30, most of the cortical tubular structures recovered close to the normal architecture, but spotty infiltration of mononuclear cells, atrophy of renal tubules and fibrosis of the interstitium remained. The control group showed no significant histological changes throughout the experimental period (data not shown).

*Apical and Lateral-Basal Localization of CD44-OX49*

To determine the localization of CD44-OX49 in rat kidneys after ATN, we performed immunohistochemistry using a purified mouse anti-rat CD44-OX49 monoclonal antibody and counterstaining for cellular nuclei with hematoxylin. In the control group, no expression of CD44-OX49 in the cortical tubular epithelial cells was found throughout the experimental period, except for a few monocytes and Bowman's capsule (data not shown). CD44-OX49 staining was markedly increased in the cortical tubular epithelial cells and infiltrating cells in the cortical interstitium and tubular lumens from the early tubular necrotic period to the later recovery period in the gentamicin group. CD44-OX49 staining was markedly increased at the lateral-basal PM in non-necrotic tubular epithelial cells, whereas it was not found on the denuded basement membrane of full necrotic tubules on day 6 after the first gentamicin administration. CD44-OX49 staining was markedly increased on the apical PM in the regenerative tubular cells on day 10, the lateral PM on day 15 and the basal PM on day 30 in the gentamicin group (fig. 1a, c, e, g). There were no positive findings in negative control samples using normal mouse IgG (data not shown).

*Lateral-Basal Localization of the CD44 Cytoplasmic Tail*

In order to prove whether CD44 localized on the apical PM was a tailless CD44 or not, we performed immunohistochemical staining using a purified rabbit anti-rat CD44CPT antibody and counterstaining for cellular nuclei with hematoxylin on serial sections. As with CD44-OX49, no expression of CD44CPT in the cortical tubular epithelial cells was found throughout the experimental period in the control group (data not shown). The CD44CPT staining was markedly increased at the lateral-basal PM in the non-necrotic tubular epithelial cells and was not localized on the denuded basement membrane of necrotic tubules on day 6 after the first gentamicin administration. The CD44CPT staining was markedly increased at lateral or lateral-basal PM on days 10 and 15 and on the basal or lateral-basal PM on day 30 in regenerative tubular epithelial cells in the gentamicin group. However, CD44CPT was not found on the apical PM in tubular epithelial cells (fig. 1b, d, f, h). There were no positive findings in negative control samples using normal rabbit IgG (data not shown).

*Change of CD44-OX49 Localization on Surface Membrane*

In order to clarify the changing process of CD44-OX49 localization from the apical to lateral-basal surface membrane in regenerative tubular epithelial cells after ATN in the gentamicin group, we performed immuno-electron microscopic examination with CD44-OX49. As a result, on day 10 after the first gentamicin administration, CD44-OX49 was mainly expressed on apical surface of the tubular basement membrane or at the newly regenerative complanate epithelial cell apex. In some tubular epithelia, CD44-OX49 was also expressed on the apical and lateral PM. On day 15, CD44-OX49 was mainly localized on the lateral PM and gradually excluded from the apical surface. Tight contact (cell-cell adhesion) between CD44-OX49-positive lateral PM of cells was generally found at that time. On day 30, CD44-OX49 was mainly localized on the basal PM and gradually excluded from the lateral surface. Finally, CD44 disappeared from basal PM when normal polarized epithelial cells formed (fig. 2).

**Fig. 2.** Change of CD44-OX49 localization from the apical to lateral-basal surface membrane in the recovery process after acute tubular necrosis. Immuno-electron microscopic examination with CD44-OX49 (**a–f**) shows that in the early recovery stage after gentamicin-induced acute tubular necrosis, CD44-OX49 is expressed on the apical surface of the tubular basement membrane (**a**) or at newly regenerative complanate epithelial cell apex (**b**). In some tubular epithelia, CD44-OX49 is expressed on the apical and lateral PM (**c**). In the middle recovery stage, CD44-OX49 is localized on the lateral PM and excluded from the apical surface (**d**). In some tubular epithelia, CD44-OX49 is expressed on the lateral and basal PM (**e**). Note the close contact (cell-cell adhesion) between the CD44-OX49-positive lateral PM of cells (**c**, **d**, **e**, arrow). In the later recovery stage, CD44-OX49 is localized on the basal PM (**f**, arrow). By that time, partial microvilli of epithelial cells have been formed (**f**, triangle). Finally, immunoelectron-microscopic examination with CD44-OX49 and lead citrate for 3 min shows that staining for CD44-OX49 disappears in the lateral and basal PM (**g**, arrow) when microvilli of normal polarized epithelial cells have been formed (**g**, triangle).

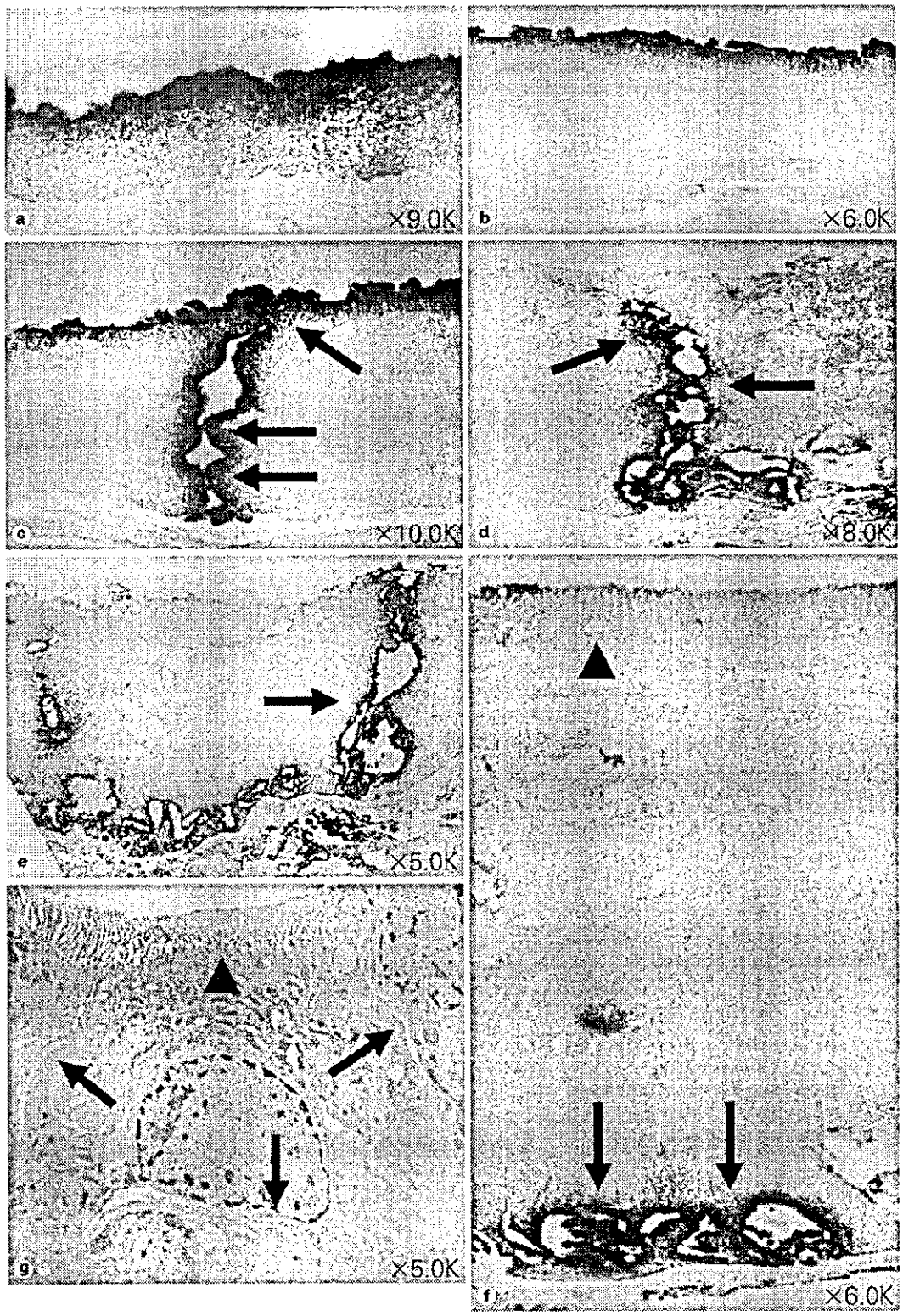
a
×9.0K
b
×6.0K
c
×10.0K
d
×8.0K
e
×5.0K
g
×5.0K
f
×6.0K

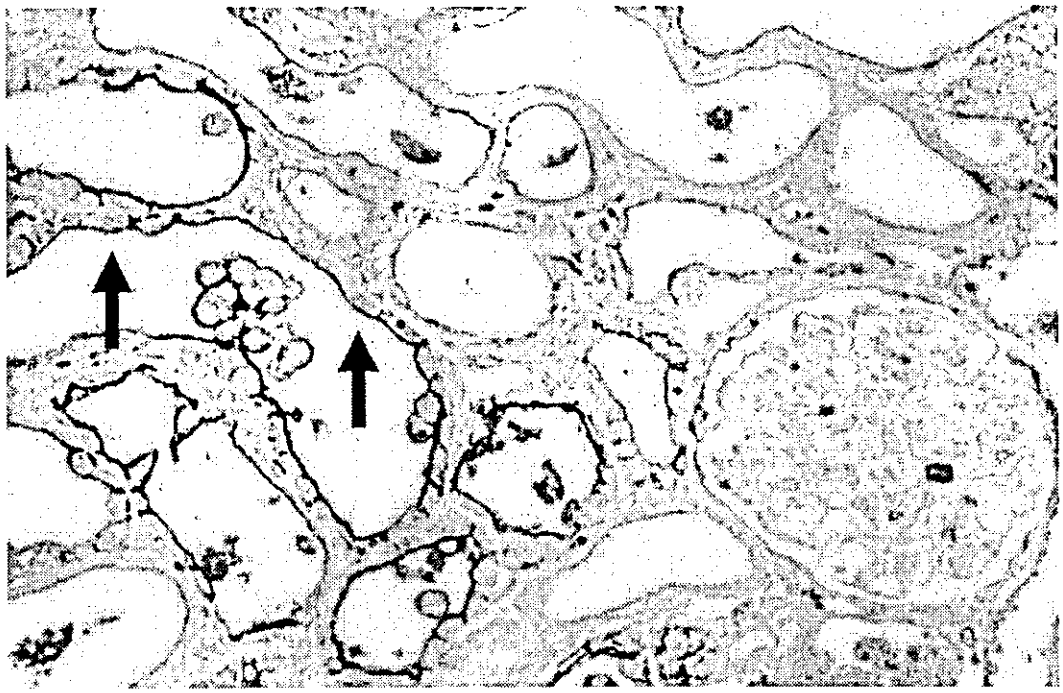

**Fig. 3.** Colocalization of CD44-OX49 on the apical surface membrane and proliferating cell nuclear antigen (PCNA) in the recovery stage after acute tubular necrosis. Note that the CD44-OX49-positive (brown) cells on the apical surface membrane are mainly PCNA-positive (red) cells, that is, newly regenerative tubular epithelial cells on day 10 after the first gentamicin injection. Original magnification × 100.

*Colocalization of CD44-OX49 on the Apical Surface Membrane and PCNA*

We demonstrated previously that the regeneration of tubular epithelial cells was most marked on day 10 after the first gentamicin injection. That is, the number of cortical tubular PCNA-positive cells reached a peak on day 10 [9]. To establish whether CD44-OX49-positive cells on the apical surface membrane were newly regenerative tubular epithelial cells or not, we carried out double staining for CD44-OX49 and PCNA as a regenerative marker. The result showed that the CD44-OX49-positive cells on the apical surface membrane were mainly PCNA-positive cells, that is, newly regenerative cells in the tubular epithelia, especially on day 10 after the first gentamicin injection (fig. 3).

*Distribution of CD44-OX49 on the Plasma Membrane in Tubular Epithelium*

In order to clarify the distribution of CD44 on epithelial cell PM in distinct stages in the gentamicin-induced ATN and recovery process, we performed quantitative analysis for localization of CD44-OX49 on tubular epithelial cell PM. The results showed that staining for CD44-OX49 was negative in full necrotic tubules on day 6 after the first gentamicin injection. On day 10, CD44-OX49 was positive on the apical PM in 68 tubules, lateral PM in 38 tubules and basal PM in 15 tubules, respectively, in 100 PCNA-positive and CD44-OX49-positive tubules. On day 15, CD44-OX49 was positive on the apical PM in 36 tubules, lateral PM in 82 tubules and basal PM in 34 tubules, respectively, in 100 CD44-OX49-positive tubules. On day 30, CD44-OX49 was positive on the apical PM in 12 tubules, lateral PM in 42 tubules and basal PM in 64 tubules, respectively, in 100 CD44-OX49-positive tubules. That is, CD44-OX49 was mainly localized to the apical PM in the early recovery stage, the lateral PM in the middle recovery stage and the basal PM in the late recovery stage after ATN (fig. 4).

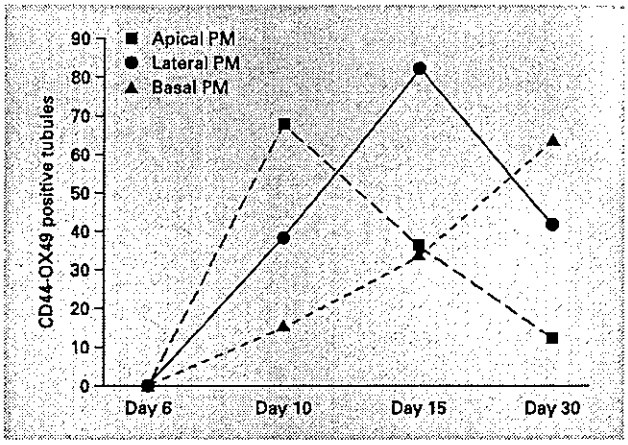


**Fig. 4.** Distribution of CD44-OX49 on the epithelial cell plasma membrane (PM) at distinct stages after acute tubular necrosis. Observations were performed on 100 non-overlapping random tubules 20 per rat kidney section from 5 rats at day 6, 10, 15 and 30 after the first gentamicin administration. The number of CD44-OX49 positive stained tubules with stained cells greater than 50% of PM was recorded. If both the basolateral PM and the apical PM were stained in greater than 50% cells these were recorded separately as basolateral PM positive and apical PM positive. Note that the CD44-OX49 is mainly localized to the apical PM in the early recovery stage, the lateral PM in the middle recovery stage and the basal PM in the late recovery stage after ATN.

## Discussion

Previous in vitro studies have demonstrated that in polarized epithelial cells, a tailless CD44 molecule is localized on the apical PM, whereas wild-type CD44 is restricted to the lateral-basal PM of epithelial cells [7]. However, in vivo studies demonstrated that CD44 is generally localized on the lateral-basal PM of renal tubular polarized epithelial cells in the kidneys, but whether it is localized on the apical PM of epithelial cells is unclear [8]. Our present in vivo study showed that CD44 was localized on not only the lateral-basal PM of renal tubular polarized epithelial cells, but also the apical PM. The staining for CD44-OX49 was positive on the apical PM in newly regenerative tubular epithelial cells in the early recovery stages after ATN, whereas staining for CD44CPT was negative. CD44CPT was only located on the lateral-basal PM. These results suggest that there were at least two types of CD44 during regeneration and repair processes after ATN. One was CD44 without a cytoplasmic tail localizing on the apical surface membrane in newly regenerative epithelial cells. Another was CD44 with a cytoplasmic tail localizing on the lateral-basal PM. Lewington et al. [8] reported that there were 4 transcripts of CD44 mRNA (4.5, 3.3, 2.0 and 1.6 kb) in kidney after acute ischemic injury in rats by Northern blot analysis. In this study, we did not perform Northern blot or Western blot analysis of CD44 because our previous study demonstrated that CD44 was located not only in renal tubular epithelial cells, but also in monocytes/macrophages in injury kidneys [9] and general Western blot could not distinguish CD44 located in renal tubules or CD44 located in monocytes/macrophages.

Both CD44 localized on the apical PM and on the lateral-basal PM were positive for immunohistochemical staining with a purified mouse anti-rat CD44-OX49 monoclonal antibody, which indicated both CD44 localized on the apical PM and CD44 localized on the lateral-basal PM might have same epitope in their distal extracellular domains. The epitope recognized by the CD44-OX49 antibody has been mapped to a region on both the standard CD44 and the splice variant isoforms of CD44 [11].

In vitro studies have demonstrated that as polarized MDCK epithelial cell cultures reach confluency, CD44 is excluded from the apical surface and becomes concentrated at areas of cell contact along the lateral cell surfaces. Additionally, in MDCK epithelial cells, both the endogenous and transfected wild-type CD44 were found on the lateral-basal surface. Deletion of the CD44 cytoplasmic tail reduces the half-life of this mutant protein and causes it to be expressed on the apical surface [7]. Confocal microscopy studies showed that CD44 indeed is expressed at the apical surface of subconfluent cultures of proximal and distal human tubular kidney cells on day 5. However, on day 9, CD44 had disappeared from the apical surface and translocated to the lateral-basal membrane [12]. These in vitro results suggest that the localization of CD44 may be regulated, and that the CD44 localized on the apical PM of epithelial cells may be CD44 without cytoplasmic domain. They may be a product of immature cells at an early stage of cell development and with a short half life. However, it has not been elucidated whether CD44 is expressed on the apical PM of epithelial cells in vivo. Our in vivo study revealed that CD44-OX49 was distinctly localized on the apical surface membrane in PCNA-positive newly regenerative epithelial cells in the early recovery stage after ATN, suggesting that it is possibly related to the regeneration of renal tubular epithelial cells. Our previous study demonstrated that a CD44 ligand, osteopontin, is related to regeneration of epithelial cells after ATN [9], this role of osteopontin might be achieved by CD44. Many studies showed that CD44

could be related to cell proliferation, regeneration and repair of injured tissues. In the facial nucleus after nerve injury and during the ensuing regeneration, strong up-regulation of CD44 on the regenerating motoneurons in the axotomized facial nucleus suggests that CD44 play a role in neurite outgrowth [13]. In the remodeling phase of healing of fractures, intense CD44 and OPN were detected in osteocytes and osteocyte lacunae, suggesting that CD44 bound to OPN plays a role in the repair of skeletal tissues [14]. In a partial hepatectomy model for studying cellular proliferation, CD44 influenced cellular differentiation, growth, cell-cell interactions and cellular polarity, and played an important role in the proliferation of residual hepatocytes and the liver regeneration [15].

Concerning localization of CD44 on lateral-basal PM, in vitro studies showed that lateral-basal targeting signals of membrane protein were localized in the cytoplasmic domain near the plasma membrane in a number of cases [1]. Mutational studies have identified $His^{330}$-$Lys^{334}$ in the cytoplasmic domain ($Asn^{290}$-$Val^{361}$) of human CD44 as a localization signal that directs membrane proteins to the lateral-basal surface. This sorting signal appears to depend critically on the integrity of the dipeptide $Leu^{331}$ and $Val^{332}$. That is, mutation of $Leu^{331}$ generated a mutant protein that was expressed on the apical PM, and mutation of $Val^{332}$ resulted in the majority of the protein being located to the lateral surface of the cells, with a residual proportion observed at the apical surface [2, 16]. However, whether or not the CD44 localized on lateral-basal PM is CD44 with a cytoplasmic domain in vivo is not clear. The present study, in which the CD44CPT was only observed at the lateral-basal PM, but not at the apical PM, confirmed for the first time that CD44 localized on the lateral-basal PM of renal tubular epithelial cells was CD44 with a cytoplasmic domain in vivo.

Although the specific mechanism was not clear, the functional significance of CD44 on the lateral-basal PM may be related to the establishment of tubular epithelial cell polarity during the recovery process after ATN. This was because adhesion and the cytoskeleton play an important role in establishment of cell polarity, and because CD44 is closely related to adhesion and the cytoskeleton. In epithelial cells, extrinsic cues from cell-cell adhesion result in the formation of cytoskeletal and signaling networks at cell contacts resulting in partial reorganization of the cells. However, full establishment of epithelial cell polarity requires both cell-cell and cell-ECM (extracellular matrix) adhesion. Specialized cytoskeletal and signaling networks assemble around adhesion receptors and position other cytoskeletal complexes and protein-sorting compartments relative to the spatial cue. In addition, binding of the cytoskeleton to adhesion receptors strengthens cell adhesion and maintains signaling from the cues [17]. The CD44 proteins are cell surface adhesion molecules involved in cell-cell and cell-matrix interactions. The principal ligand of CD44 is hyaluronic acid, an integral component of the ECM. Other CD44 ligands include osteopontin, serglycin, collagens, fibronectin, and laminin [4]. Kalomiris and Bourguignon [18] demonstrated that CD44 is a transmembrane protein with a cytoplasmic domain that binds directly to ankyrin, a molecule known to link the membrane to the cytoskeleton. Ankyrin plays a specific role in membrane skeleton organization, ionic transport, and maintenance of cell polarity, as well as cell-cell adhesion regulation. The interaction between the membrane skeleton and cytoplasmic domains of transmembrane proteins plays a fundamental role in membrane integrity and stability, as well as in many other cellular processes [19]. In addition, the CD44 cytoplasmic domain also can directly bind to ERM family members (ezrin, radixin, and moesin), which are crucial components that provide a regulated linkage between membrane proteins and the cortical cytoskeleton, as well as participating in signal-transduction pathways [6, 20, 21]. Our in vivo results showed that CD44 was expressed distinctly on the lateral PM and in close contact with lateral PM between cells (cell-cell adhesion) in the middle stage of epithelial cell repair after ATN. In the late stage of epithelial cell repair, CD44 was mainly located to the basal PM. By that time, epithelial cell polarity had been basically established, evidenced by initial microvilli appearance in the apical surface membrane. After full establishment of epithelial cell polarity, CD44 disappeared from the basal surface membrane. These results suggest CD44 is related to the establishment of epithelial cell polarity.

In summary, we used a gentamicin-induced ATN and spontaneous recovery model in rats and two distinct antibodies and surveyed the localization of CD44-OX49 and CD44CPT on the PM in renal tubular epithelial cells in the recovery process after ATN with immunohistochemistry and immunoelectron-microscopic examination. The present study provided the following new in vivo evidence. First, CD44-OX49 was localized not only on the lateral-basal PM of renal tubular epithelial cells, but also on the apical PM in PCNA-positive newly regenerative tubular epithelial cells in the early recovery stages after ATN, whereas CD44CPT was localized only on the lateral-basal PM in vivo. Second, localization of CD44 was changed from the apical to lateral to basal PM in renal tubular epithelial cells during the recovery process after

ATN, and finally disappeared from the basal surface membrane when normal polarized epithelial cells formed in vivo. These results suggest that there were two types of CD44, with and without a cytoplasmic tail, with different localization during the recovery process after ATN. The CD44 localized on the apical surface membrane might have been CD44 without a cytoplasmic tail which could be related to the regeneration of epithelial cells, whereas the CD44 localized on the lateral and basal PM might have been CD44 with a cytoplasmic tail which could participate in establishment of tubular epithelial cell polarity by adhesion and binding of cytoskeletal associated proteins.


## Acknowledgements

This work was supported in part by a Health and Labour Science Research Grant for Research on Specific Diseases from the Ministry of Health, Labour and Welfare, and by a Grant-in-Aid for Scientific Research (C, No. 11671032) from the Ministry of Education, Culture, Sports, Science and Technology of Japan. An abstract of this work was presented at the 44th Annual Meeting of the Japanese Society of Nephrology (Tokyo, Japan, 2001) and the 2001 ASN/ISN World Congress of Nephrology (San Francisco, Calif., USA, 2001), respectively.


## References


1 Matter K, Mellman I: Mechanisms of cell polarity: Sorting and transport in epithelial cells. Curr Opin Cell Biol 1994;6:545–554.
2 Sheikh H, Isacke CM: A di-hydrophobic Leu-Val motif regulates the lateral-basal localization of CD44 in polarized Madin-Darby canine kidney epithelial cells. J Biol Chem 1996;271:12185–12190.
3 Xie Y, Sakatsume M, Nishi S, Narita I, Arakawa M, Gejyo F: Expression, roles, receptors, and regulation of osteopontin in the kidney. Kidney Int 2001;60:1645–1657.
4 Goodison S, Urquidi V, Tarin D: CD44 cell adhesion molecules. Mol Pathol 1999;52:189–196.
5 Lesley J, Hyman R: CD44 structure and function. Front Biosci 1998;3:D616–630.
6 Tsukita S, Oishi K, Sato N, Sagara J, Kawai A, Tsukita S: ERM family members as molecular linkers between the cell surface glycoprotein CD44 and actin-based cytoskeletons. J Cell Biol 1994;126:391–401.
7 Neame SJ, Isacke CM: The cytoplasmic tail of CD44 is required for lateral-basal localization in epithelial MDCK cells but does not mediate association with the detergent-insoluble cytoskeleton of fibroblasts. J Cell Biol 1993;121:1299–1310.
8 Lewington AJ, Padanilam BJ, Martin DR, Hammerman MR: Expression of CD44 in kidney after acute ischemic injury in rats. Am J Physiol 2000;278:R247–R254.
9 Xie Y, Nishi S, Iguchi S, Imai N, Sakatsume M, Saito A, Ikegame M, Iino N, Shimada H, Ueno M, Kawashima H, Arakawa M, Gejyo F: Expression of osteopontin in gentamicin-induced acute tubular necrosis and its recovery process. Kidney Int 2001;59:959–974.
10 Gunthert U, Hofmann M, Rudy W, Reber S, Zoller M, Haussmann I, Matzku S, Wenzel A, Ponta H, Herrlich P: A new variant of glycoprotein CD44 confers metastatic potential to rat carcinoma cells. Cell 1991;65:13–24.
11 Arch R, Wirth K, Hofmann M, Ponta H, Matzku S, Herrlich P, Zoller M: Participation in normal immune responses of a metastasis-inducing splice variant of CD44. Science 1992;257:682–685.
12 Verhulst A, Asselman M, Persy VP, Schepers MS, Helbert MF, Verkoelen CF, De Broe ME: Crystal retention capacity of cells in the human nephron: Involvement of CD44 and its ligands hyaluronic acid and osteopontin in the transition of a crystal binding into a nonadherent epithelium. J Am Soc Nephrol 2003;14:107–115.
13 Jones LL, Kreutzberg GW, Raivich G: Regulation of CD44 in the regenerating mouse facial motor nucleus. Eur J Neurosci 1997;9:1854–1863.
14 Yamazaki M, Nakajima F, Ogasawara A, Moriya H, Majeska RJ, Einhorn TA: Spatial and temporal distribution of CD44 and osteopontin in fracture callus. J Bone Joint Surg Br 1999;81:508–515.
15 Della Fazia MA, Pettirossi V, Ayroldi E, Riccardi C, Magni MV, Servillo G: Differential expression of CD44 isoforms during liver regeneration in rats. J Hepatol 2001;34:555–561.
16 Stamenkovic I, Amiot M, Pesando JM, and Seed B: A lymphocyte molecule implicated in lymph node homing is a member of the cartilage link protein family. Cell 1989;56:1057–1062.
17 Drubin DG, Nelson WJ: Origins of cell polarity. Cell 1996;84:335–344.
18 Kalomiris EL, Bourguignon LY: Mouse T lymphoma cells contain a transmembrane glycoprotein (GP85) that binds ankyrin. J Cell Biol 1988;106:319–327.
19 Hryniewicz-Jankowska A, Czogalla A, Bok E, Sikorsk AF: Ankyrins, multifunctional proteins involved in many cellular pathways. Folia Histochem Cytobiol 2002;40:239–249
20 Nakamura H, Ozawa H: Immunolocalization of CD44 and the ERM family in bone cells of mouse tibiae. J Bone Miner Res 1996;11:1715–1722.
21 Nakamura H, Ozawa H: Immunolocalization of CD44 and the ezrin-radixin-moesin (ERM) family in the stratum intermedium and papillary layer of the mouse enamel organ. J Histochem Cytochem 1997;45:1481–1492.

Available online at www.sciencedirect.com
SCIENCE DIRECT®
Biochemical and Biophysical Research Communications 317 (2004) 1103–1107
BBRC
www.elsevier.com/locate/ybbrc

# Gene expression profile of human mesenchymal stem cells during osteogenesis in three-dimensional thermoreversible gelation polymer

Keiichi Hishikawa,[a,b,d,*] Shigeki Miura,[c] Takeshi Marumo,[a,b,d] Hiroshi Yoshioka,[c] Yuichi Mori,[c] Tsuyoshi Takato,[d] and Toshiro Fujita[a,b]

[a] *Department of Clinical Renal Regeneration, Graduate School of Medicine, University of Tokyo, Japan*
[b] *Department of Nephrology and Endocrinology, University of Tokyo, Japan*
[c] *Mebiol Inc., Japan*
[d] *Division of Tissue Engineering, The University of Tokyo Hospital, Japan*

Received 8 March 2004

**Abstract**

This study attempted to characterize the ability of thermoreversible gelation polymer (TGP) to induce differentiation of human mesenchymal stem cells (hMSC) into osteoblasts. Using a long oligo microarray system consisting of 3760 genes, we compared the expression profiles of the cells in 2-dimensional (2D) culture, 3D culture in collagen gel, and 3D culture in TGP with or without osteogenic induction. Compared to 2D culture, the gene expression profile of hMSC showed almost the same pattern in TGP without osteogenic induction, but 72% of genes (2701/3760) were up-regulated in collagen gel. With osteogenic induction, hMSC showed higher ALP activity and osteocalcin production in TGP as compared to 2D culture. Moreover, up-regulation and down-regulation of osteogenic genes were augmented in 3D culture in TGP as compared to 2D culture. As TGP is chemically synthesized and completely free from pathogen such as prion in bovine spongiform encephalopathy, these results suggest that TGP could be applied clinically to induce osteogenic differentiation of hMSC.


*Keywords:* Stem cell; Osteogenesis; Human mesenchymal stem cell; DNA microarray; Polymer

Human bone marrow mesenchymal stem cells (hMSC) can selectively differentiate into osteogenic, chondrogenic, or adipogenic lineages depending on the conditions of the medium in which they are cultured. When hMSC are cultured with dexamethasone, ascorbic acid-2-phosphate, and β-glycerophosphate, they differentiate into an osteogenic lineage and form mineral [1].

There is a large difference between a flat layer of cells and a complex 3-dimensional (3D) tissue, and the development of biological materials for 3D culture is a key area in regenerative medicine. For 3D culture, many researchers have used collagen gel [2] or "Matrigel" [3], but these materials are prepared from bovine or mouse tumors and are not appropriate for clinical use. To avoid infection in clinical use, chemically synthesized biocompatible polymer is an ideal material. Thermoreversible gelation polymer (TGP) [4] is a biocompatible polymer and is completely free from pathogen such as prion in bovine spongiform encephalopathy [5].

In this study, we examined the osteogenic differentiation of hMSC in TGP and compared comprehensive gene expression with that in a 2D culture system. We report here that osteogenic differentiation was augmented in 3D culture in TGP, and TGP is a potential clinical biomaterial for bone regeneration from hMSC.

## Materials and methods

*Cell culture.* Cryopreserved hMSC from a single donor and their required basal medium and growth supplements were purchased from

* Corresponding author. Fax: +81-3-5800-9738.
*E-mail address:* hishikawa-tky@umin.ac.jp (K. Hishikawa).

0006-291X/$ - see front matter © 2004 Elsevier Inc. All rights reserved.
doi:10.1016/j.bbrc.2004.03.165

BioWhittaker (Walkersville, MD). Osteogenic medium was also purchased from BioWhittaker. TGP was purchased from Mebiol (Tokyo, Japan). Collagen gel (type I) was purchased from KOKEN (Tokyo, Japan). For TGP preparation, 10 ml of control or osteogenic medium was added to TGP in a T25 flask 24 h before use. On day 0, cells were seeded at a density of $3.0 \times 10^3$ cells/cm$^2$ (2D culture) or $3.0 \times 10^3$ cells/ml of TGP (3D culture). The next day, the culture medium was replaced with osteogenic medium, and the medium was changed twice a week until day 14.

*Microarray analysis.* DNA microarray hybridization experiments were performed using Clontech Atlas glass human 3.8 (BD Bioscience) according to the manufacturer's protocol. The protocol and the complete list of genes can be viewed at http://www.bdbiosciences.com/clontech/techinfo/manuals/index.shtml. The DNA arrays were scanned using GenePix4000A [6].

*Measurement of ALP activity, calcium deposition, and osteocalcin.* ALP activity was measured using an ALP measurement kit (ALP-K Test; Wako Chemicals) [7]. Osteocalcin was determined using an osteocalcin-immunofluorescence kit (BACHEM AG).

*Histochemical staining.* After 14 days of culture, cells were washed twice with PBS and fixed with 10% PFA for 10 min at room temperature. Fixed cells were stained with 5% silver nitrate (Nakarai) for von Kossa staining [8].

## Results

### *Microarray analysis in 3D culture*

In mammalian tissues, cells connect not only with each other, but also with a support structure called the extracellular matrix (ECM). ECM contains collagen, elastin, laminin, fibronectin, etc., and these proteins contain specific motifs that are particularly favorable for cell attachment and function. On the other hand, TGP contains no such motifs as a scaffold, and nothing is known as to whether this affects cell function or not. When hMSC are cultured in control medium in 2D culture, they slowly proliferate without differentiation. Accordingly, we examined the gene expression profile of hMSC cultured in 3D culture (TGP and collagen gel) in control medium. In TGP culture, scattered plots of gene expression were evenly distributed in both the upper left (1959 genes: 52%) and lower right (1801 genes: 48%) areas. On the other hand, scattered plots of gene

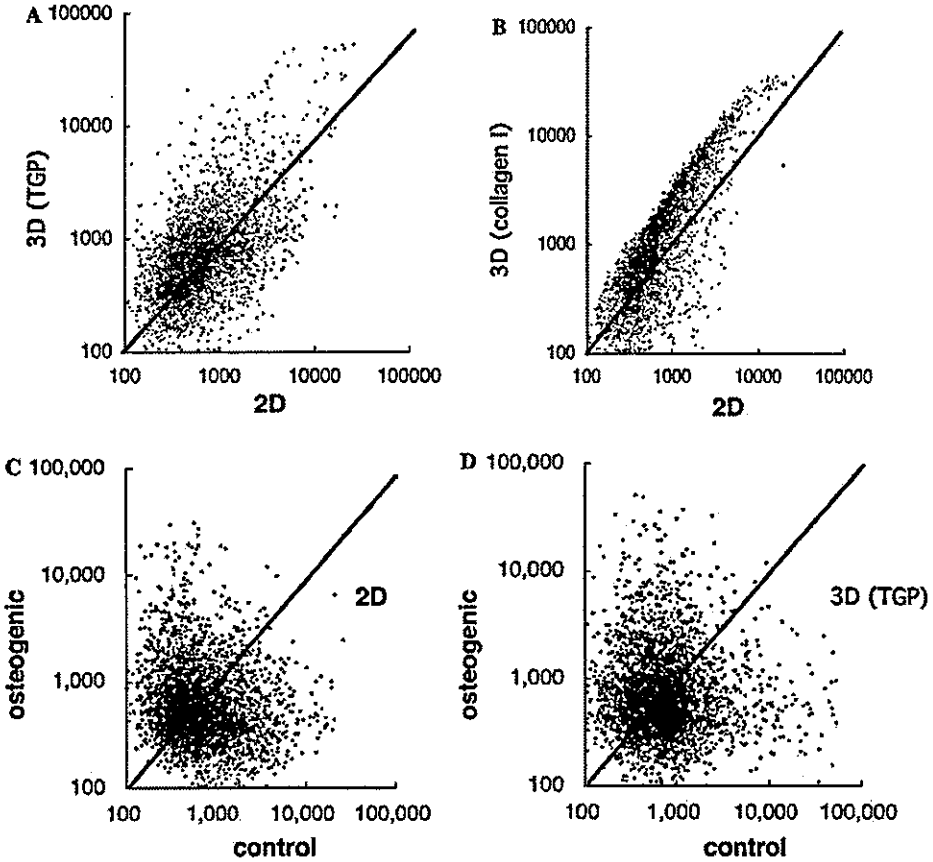


Fig. 1. Scatter-plot analyses of gene expression of hMSC in various culture conditions. (A) 3D culture in TGP vs. 2D culture without induction. (B) 3D culture in collagen gel vs. 2D culture without induction. (C) Osteogenic medium vs. control medium in 2D culture. (D) Osteogenic medium vs. control medium in 3D TGP culture.

expression in collagen gel were mainly distributed in the upper left (2701 genes: 72%), indicating that collagen gel itself stimulated gene expression of hMSC without any induction.

Next, we examined the gene expression profile of hMSC in osteogenic culture medium for 14 days. In 2D culture, unexpectedly, scattered plots of gene expression were evenly distributed in both the upper left (2026 genes: 53.8%) and lower right (1734 genes: 47%) areas, and this was also the case in TGP culture with osteogenic medium (1896 and 1864 genes, respectively).

*Matrix mineralization and osteocalcin production*

Next, we confirmed whether osteogenic differentiation could be induced in 3D culture in TGP. Human MSC were cultured in 2D or TGP with osteogenic medium for 14 days, and osteogenic differentiation was demonstrated by mineralization stained using the von Kossa method. As shown in Figs. 2A and B, much more mineral was produced in TGP as compared to 2D culture. Moreover, ALP activity [9] and osteocalcin production were significantly higher in TGP as compared to 2D culture (Figs. 2C and D).

*Up-regulation and down-regulation of osteogenic genes in TGP*

Among 3760 genes, we examined the up-regulation of typical osteogenic genes such as type I collagen [9], alkaline phosphatase [10], osteocalcin [11], and osteopontin [12]. Moreover, recent genome-wide screening by means of a cDNA microarray system consisting of 23,040 genes revealed that 55 genes were up-regulated and 82 genes were down-regulated in hMSC during osteogenic differentiation [13]. We also examined the expression of several of these genes (metallothionetin 2A, osteoprotegrin, dual specificity phosphatase 6,

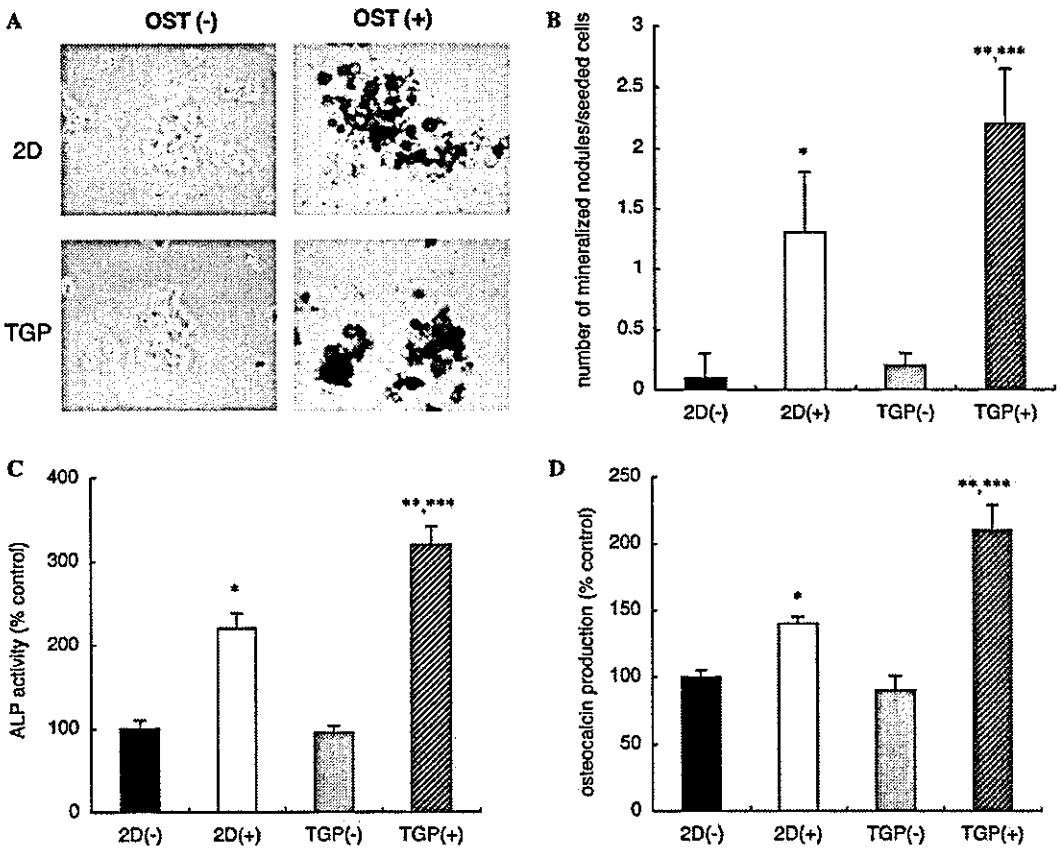


Fig. 2. (A) von Kassa staining without induction (−) and with osteogenic induction (+) in 2D and 3D culture in TGP. (B) von Kossa histomorphometric analysis. Deposition of calcified extracellular matrix (von Kossa staining) was significantly greater with osteogenic induction in both 2D culture and 3D culture in TGP. Deposition was significantly enhanced in TGP compared with 2D culture. (C) Assay for alkaline phosphatase (ALP) activity. ALP activity was significantly higher with osteogenic induction in both 2D culture and 3D culture in TGP. ALP activity was significantly enhanced in TGP compared with 2D culture. (D) Osteocalcin production. Osteocalcin production was significantly higher with osteogenic induction in both 2D culture and 3D culture in TGP. Osteocalcin production was significantly enhanced in TGP compared with 2D culture. $^{*}p < 0.05$: 2D(−) vs. 2D(+). $^{**}p < 0.05$: TGP(−) vs. TGP(+). $^{***}p < 0.05$: 2D(+) vs. TGP(+).

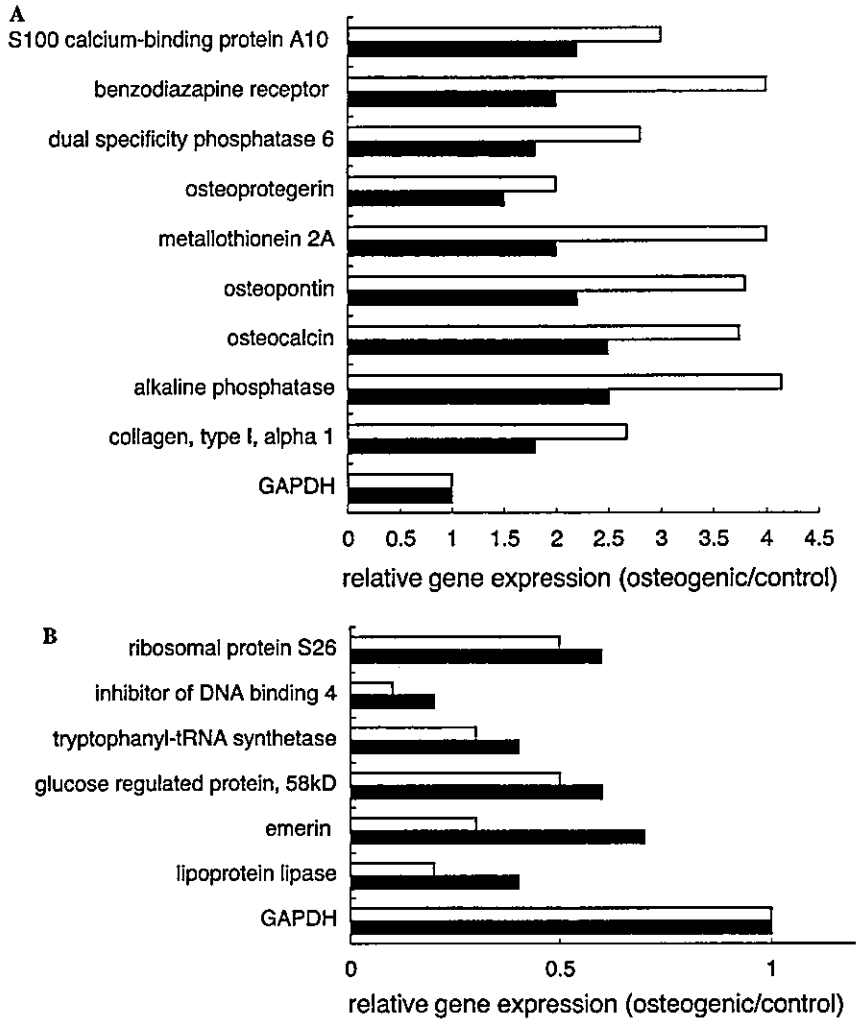


Fig. 3. Osteogenic gene expression in 2D culture and 3D culture in TGP. (A) Genes up-regulated by osteogenic induction. (B) Genes down-regulated by osteogenic induction. Fold change represents the ratio of signal intensity (expression in osteogenic medium/expression in control medium). Closed bars represent 2D culture and open bars represent 3D culture in TGP.

benzodiazapine receptor, S100 calcium binding protein A10, lipoprotein lipase, emerin, glucose-regulated protein 58 kDa, tryptophanyl-tRNA synthetase, inhibitor of DNA binding 4, and ribosomal protein S26) in TGP with osteogenic medium. As shown in Fig. 3, up- or down-regulation of all these genes was augmented in 3D culture in TGP as compared to 2D culture.

## Discussion

3D culture techniques are expected to play a key role in regenerative medicine, especially in the field of tissue engineering, but several conditions are required for the culture material. First, it should be free from pathogens such as prion. Collagen gels are usually made from bovine tissue, and it is impossible to rule out the possibility of BSE completely. Matrigel is made from animal tumors. On the other hand, TGP is a chemically synthesized material and completely free from pathogens. Second, to optimize the conditions for lineage-specific differentiation, the material should be able to keep stem cells in an inactive stable condition without induction. Matrigel contains several unidentified growth factors. Collagen gel alone activated gene expression of hMSC without any induction, but TGP did not (Fig. 1). These results suggest that TGP is applicable as a 3D material for clinical regenerative medicine.

Recently, Doi et al. analyzed the gene expression profile during the mineralization process of hMSC by means of a cDNA microarray system consisting of

23,040 genes, and confirmed up-regulation of 55 genes and down-regulation of 82 genes. As shown in Fig. 3, we also confirmed up- or down-regulation of several of these genes during mineralization, but the roles of these genes remain to be determined. It is interesting that ALP activity and osteocalcin production were augmented in 3D culture in TGP compared to 2D culture. During osteogenic induction, it is possible that hMSC may produce some humoral factors that contribute to osteogenic differentiation in an autocrine manner. We speculate that augmentation of osteogenic induction was caused by a high local concentration of these factors with TGP culture. TGP is composed of poly(*N*-isopropylacrylamide-co-*n*-butyl methacrylate) [poly(NIPAAm-co-BMA)] and polyethylene glycol (PEG), and has thermoreversible fine crosslinks between intermolecular poly(NIPAAm-co-BMA) blocks due to hydrophobic interaction [4]. This structure makes it possible to vary the diffusive speed according to the character of the molecules. According to the formula of Lee et al. [14], the diffusive speeds of phenol red (small hydrophilic molecule), myoglobin (large hydrophilic molecule), and methylene blue (small hydrophobic molecule) are calculated as $1.6 \times 10^{-6}$, $2.1 \times 10^{-7}$, and $7.5 \times 10^{-9}$ cm$^2$/s, respectively. Thus, TGP may be able to maintain a high local concentration of hydrophobic molecules and hydrophilic large molecules, and this creates a concentration gradient of each molecule. It is possible that this concentration gradient in TGP may act as a morphogen gradient [15] in vivo and augment osteogenic induction in hMSC.

In summary, 3D culture in TGP is able to maintain hMSC in a stable inactive condition without induction and augment osteogenic differentiation of hMSC cultured with dexamethasone, ascorbic acid-2-phosphate, and β-glycerophosphate. TGP is completely free from prion and may be able to induce a morphogen gradient in the differentiation process in 3D culture. Our results suggest the possible clinical application of TGP for regenerative medicine, especially for bone regeneration by hMSC.

## Acknowledgments

This study was supported by a grant from the Open Competition for the Development of Innovative Technology and the Mochida Pharmaceutical Co. Ltd.

## References

[1] M.F. Pittenger, A.M. Mackay, S.C. Beck, R.K. Jaiswal, R. Douglas, J.D. Mosca, M.A. Moorman, D.W. Simonetti, S. Craig, D.R. Marshak, Multilineage potential of adult human mesenchymal stem cells, Science 284 (1999) 143–147.

[2] A. Islam, R. Steiner, Primary culture of marrow core in collagen gels: modulation and transformation of endosteal cells. I. Morphologic observations, J. Med. 20 (1989) 241–250.

[3] H.K. Kleinman, M.L. McGarvey, L.A. Liotta, P.G. Robey, K. Tryggvason, G.R. Martin, Isolation and characterization of type IV procollagen, laminin, and heparan sulfate proteoglycan from the EHS sarcoma, Biochemistry 21 (1982) 6188–6193.

[4] H. Yoshioka, M. Mikami, Y. Mori, E. Tsuchida, A synthetic hydrogel with thermoreversible gelation, J. Macromol. Sci. A 31 (1994) 113–120.

[5] S.B. Prusiner, Biology and genetics of prion diseases, Annu. Rev. Microbiol. 48 (1994) 655–686.

[6] K. Hishikawa, B.S. Oemar, T. Nakaki, Static pressure regulates connective tissue growth factor expression in human mesangial cells, J. Biol. Chem. 276 (2001) 16797–16803.

[7] K. Shindo, N. Kawashima, K. Sakamoto, A. Yamaguchi, A. Umezawa, M. Takagi, K. Katsube, H. Suda, Osteogenic differentiation of the mesenchymal progenitor cells, Kusa is suppressed by Notch signaling, Exp. Cell Res. 290 (2003) 370–380.

[8] J.L. Dragoo, J.Y. Choi, J.R. Lieberman, J. Huang, P.A. Zuk, J. Zhang, M.H. Hedrick, P. Benhaim, Bone induction by BMP-2 transduced stem cells derived from human fat, J. Orthop. Res. 21 (2003) 622–629.

[9] M. Sandberg, H. Autio-Harmainen, E. Vuorio, Localization of the expression of types I, III, and IV collagen, TGF-beta 1 and c-fos genes in developing human calvarial bones, Dev. Biol. 130 (1988) 324–334.

[10] G.R. Beck Jr., E.C. Sullivan, E. Moran, B. Zerler, Relationship between alkaline phosphatase levels, osteopontin expression, and mineralization in differentiating MC3T3-E1 osteoblasts, J. Cell. Biochem. 68 (1998) 269–280.

[11] G.S. Stein, J.B. Lian, Molecular mechanisms mediating proliferation/differentiation interrelationships during progressive development of the osteoblast phenotype, Endocr. Rev. 14 (1993) 424–442.

[12] M.A. Dorheim, M. Sullivan, V. Dandapani, X. Wu, J. Hudson, P.R. Segarini, D.M. Rosen, A.L. Aulthouse, J.M. Gimble, Osteoblastic gene expression during adipogenesis in hematopoietic supporting murine bone marrow stromal cells, J. Cell. Physiol. 154 (1993) 317–328.

[13] M. Doi, A. Nagano, Y. Nakamura, Genome-wide screening by cDNA microarray of genes associated with matrix mineralization by human mesenchymal stem cells in vitro, Biochem. Biophys. Res. Commun. 290 (2002) 381–390.

[14] E.K.L. Lee, H.K. Lonsdale, R.W. Baker, E. Drioli, P.A. Bresnahan, Transport of steroids in poly(etherurethane) and poly(ethylene vinyl acetate) membranes, J. Membr. Sci. 24 (1985) 125–143.

[15] J.B. Gurdon, P.Y. Bourillot, Morphogen gradient interpretation, Nature 413 (2001) 797–803.

Available online at www.sciencedirect.com
SCIENCE DIRECT®
Biochemical and Biophysical Research Communications 319 (2004) 103–113
BBRC
www.elsevier.com/locate/ybbrc

# Sall1, a causative gene for Townes–Brocks syndrome, enhances the canonical Wnt signaling by localizing to heterochromatin

Akira Sato,[a,b] Shosei Kishida,[c] Toshiya Tanaka,[d] Akira Kikuchi,[c] Tatsuhiko Kodama,[d] Makoto Asashima,[b] and Ryuichi Nishinakamura[a,e,f,*]

[a] *Division of Stem Cell Regulation, The Institute of Medical Science, The University of Tokyo, Tokyo 108-8639, Japan*
[b] *Department of Life Sciences, The University of Tokyo, Tokyo 153-8902, Japan*
[c] *Department of Biochemistry, Faculty of Medicine, Hiroshima University 1-2-3, Kasumi, Minami-ku, Hiroshima 734-8551, Japan*
[d] *Laboratory for Systems Biology and Medicine, Research Center for Advanced Science and Technology, The University of Tokyo, Tokyo 153-8904, Japan*
[e] *Division of Integrative Cell Biology, Institute of Molecular Embryology and Genetics, Kumamoto University, Kumamoto 860-0811, Japan*
[f] *PREST, JST, Saitama 332-0012, Japan*

Received 12 April 2004

**Abstract**

The *Spalt* (*sal*) gene family plays an important role in regulating developmental processes of many organisms. Mutations of human *SALL1* cause the autosomal dominant disorder, Townes–Brocks syndrome (TBS), and result in ear, limb, anal, renal, and heart anomalies. Targeted deletion of mouse *Sall1* results in kidney agenesis or severe dysgenesis. Molecular mechanisms of *Sall1*, however, have remained largely unknown. Here we report that Sall1 synergistically activates canonical Wnt signaling. The transcriptional activity of Sall1 is related to its nuclear localization to punctate nuclear foci (pericentromeric heterochromatin), but not to its localization or association with β-catenin, the nuclear component of Wnt signaling. In contrast, the RNA interference of Sall1 reduces reporter activities of canonical Wnt signaling. The N-terminal truncated Sall1, produced by mutations often found in TBS, disturbs localization of native Sall1 to heterochromatin, and also down-regulates the synergistic transcriptional enhancement for Wnt signal by native Sall1. Thus, we propose a new mechanism for Wnt signaling activation, that is the heterochromatin localization of Sall1.


The *Spalt* (*sal*) gene family plays important roles in regulating developmental processes of many organisms. In *Drosophila* development, *sal* is a region-specific homeotic gene, which specifies cell fate decisions of chordontonal precursors in the peripheral nervous system [1,2], regulates tracheal development [3], controls terminal differentiation of photoreceptors [4], and determines proper placement of wing veins [5,6].

Humans have four *sal* related genes (*SALL1*, *SALL2*, *SALL3*, and *SALL4*) and mice also have four (*Sall1*, *Sall2*, *Sall3*, and *Sall4*) [7–15]. Heterozygous mutations of human *SALL1* lead to Townes–Brocks syndrome, with features of dysplastic ears, preaxial polydactyly, imperforate anus, and (less commonly) kidney and heart anomalies [16]. With homozygous deletion in mice the kidney had severe defects which meant that *Sall1* has an essential role in kidney development [17]. The molecular mechanisms of Sall1 have remained obscure.

*Sall1* encodes a protein that contains 10 zinc finger motifs. The most N-terminal zinc finger is a single C2HCtype and is conserved only in vertebrates (*Drosophila sal* does not have the N-terminal C2HC zinc finger) [18]. The other zinc fingers are of the C2H2-type and are arranged as doublets with a third finger associated with the second pair. Recently, it was reported that Sall1 functions as a transcriptional repressor, by being localized to pericentromeric heterochromatin and is associated with histone deacetylase (HDAC) complex [19,20]. When linked to a heterologous DNA-binding

* Corresponding author. Fax: +81-96-373-6618.
*E-mail address:* ryuichi@kaiju.medic.kumamoto-u.ac.jp (R. Nishinakamura).

0006-291X/$ - see front matter © 2004 Elsevier Inc. All rights reserved.
doi:10.1016/j.bbrc.2004.04.156